Journal of Institute of Science and Technology, 24(2), 44-48 (2019)
ISSN: 2469-9062 (print), 2467-9240 (e)
Doi: http://doi.org/10.3126/jist.v24i2.27256

Research Article

EFFECT OF POTASSIUM NITRATE IN ZnO NANOPARTICLE SYNTHESIS TO STUDY THE PERFORMANCE OF DYE SENSITIZED SOLAR CELL

Leela Pradhan Joshi[1], Jeny Bhatta[1], Tika Bahadur Katuwal[2], Bhim Prasad Kafle[3], Deependra Das Mulmi[4*]

[1]Department of Physics, Amrit Campus, Tribhuvan University, Kathmandu, Nepal
[2]Department of Physics, Tri-Chandra Multiple Campus, Tribhuvan University, Kathmandu, Nepal
[3]Department of Chemical Science and Engineering, Kathmandu University, Dhulikhel, Nepal
[4]Nanomaterials Research Laboratory, Nepal Academy of Science and Technology, Khumaltar, Nepal
[*]Corresponding author: deependra.mulmi@nast.gov.np

*(**Received**: November 7, 2019; **Revised**: December 11, 2019; **Accepted**: December 20, 2019)*

ABSTRACT

X-ray diffraction, Raman investigations, band gap energy of zinc oxide nanoparticles (ZnO NPs) along with current-voltage characteristic curves of an assembled dye-sensitized solar cell (DSSC) are presented in this article. ZnO NPs were first synthesized with and without potassium nitrate (KNO_3) salt by precipitation method from precursor solutions of zinc acetate and sodium hydroxide. Then, their thin films were deposited on FTO substrates from the paste made with acetic-acid glacial, and Triton X-100 in ethanol by doctor blade method. The X-ray diffraction (XRD) pattern of ZnO NPs prepared without KNO_3 annealed at 500 °C showed a hexagonal wurtzite structure with preferred orientation along (101) planes and crystallite size of 25 nm. Very similar XRD pattern was found for ZnO NPs prepared with KNO_3. The crystallite size was found decreased to 17 nm for ZnO NPs made with KNO_3 salt. Raman spectrum of ZnO NPs showed the presence of E_2 high or $E_2(2)$ peak at 437 cm^{-1}. The optical band gaps of the ZnO thin films prepared from ZnO NPs with and without KNO_3 were measured to be of 3.16 eV and 3.26 eV, respectively. After sensitizing the above-prepared ZnO films by dye extract of *Artocarpus lakoocha*, the dye-sensitized solar cells were prepared, and their performance was tested by measuring I-V curves under light illumination of the power density of 1000 W/m^2. The measurement showed highest I_{sc} and V_{oc} of 44 μA and 326 mV, respectively.

Keywords: Band gap energy, Dye-sensitized solar cell, Raman spectrum, X-ray diffraction, ZnO nanoparticles

INTRODUCTION

To meet today's high energy demand, research on the fabrication of various types of solar cells has been progressing tremendously. One such type is dye-sensitized solar cell (DSSC) whose fabrication along with its future scope increasing because of its real economic processing cost and less hazardous by-products compared to other silicon-based and thin-film solar cells. In DSSC, the size and the quality of metal oxide semiconducting layer made up of titanium oxide (TiO_2) or zinc oxide (ZnO) play a vital role in enhancing its performance (Al-Kahlout, 2015). In recent years, zinc oxide nanoparticles (ZnO NPs) have been used as a potential compound semiconducting material in dye-sensitized solar cell technology (Chu *et al.*, 2009; Sharma *et al.*, 2017) because of their excellent properties such as high transparency, large optical band gap (3.3 eV), high electron mobility (100 $cm^2V^{-1}s^{-1}$), large exciton binding energy (60 meV), strong room-temperature uminescence and high chemical and thermal stability (Ghimire *et al.*, 2015; Chen & Lo, 2011; Suh *et al.*, 2007). The ZnO NPs and their corresponding thin films have a large number of applications such as solar cells, veristors, gas sensors, thin-film transistors, UV photodetectors, and light-emitting diodes (Plank *et al.*, 2009; Chatterjee *et al.*, 1999). The ZnO nanoparticles and their thin films can be synthesized employing various processes: sonochemical, solid-state pyrolytic reaction, hydrothermal, magnetron sputtering (Yadav *et al.*, 2008; Wang *et al.*, 2003; Ramimoghadam *et al.*, 2012; Srivastava *et al.*, 2010). One of the most cost-effective and efficient methods is the precipitation method (Ghorbani *et al.*, 2015; Panthi *et al.*, 2018). This article reports on the preparation of ZnO NPs by the precipitation method from the precursor solutions of zinc acetate and sodium hydroxide along with the addition of potassium nitrate to study the additive effect on the crystallite size of ZnO NPs and its impact on the performance of DSSC. The execution of dye-sensitized solar cells was measured using the above-prepared ZnO electrode sensitized by natural dye extract of leaves of *Artocarpus lakoocha* commonly known as monkey fruit collected from Dhangadi, far western part of Nepal.

MATERIALS AND METHODS

A schematic diagram (Fig. 1) indicates the experimental procedure for the preparation of ZnO NPs. First of all, 0.5 M solution of zinc acetate dihydrated in ethanol was prepared with continuous stirring for 1 h at 60° C for the preparation of precursor-A. Similarly, 0.9 M solution of sodium hydroxide in ethanol (precursor-B) was prepared by stirring continuously for the same period and at same

temperature. After complete dissolution of solutes in their respective solvents, sodium hydroxide solution (B) was added drop-wise in the zinc acetate solution (A), for one hour, with vigorous stirring. The mixture solution of A and B was left overnight to settle zinc hydroxide precipitate. The precipitate was then centrifuged at 1100 rpm for 10 minutes to remove the excess mother liquor. This process was repeated four times, followed by aqueous washing and finally with ethanol to remove any by-product which might have bound to the ZnO NPs. Subsequently, the yield was annealed at high temperature of 500° C for 2 h at which $Zn(OH)_2$ was decomposed into ZnO NPs.

Following the same procedure, the ZnO NPs was prepared by adding KNO_3 salt solution into the precursor-A with a molar ratio of 1:1 to study the effect of KNO_3 into the ZnO NPs synthesis. A thin layer of ZnO was then deposited on a transparent and conducting fluorine-doped tin oxide (FTO) glass substrates using doctor blade method for which ZnO paste was prepared by mixing above prepared ZnO NPs with acetic acid glacial, Triton X-100 and ethanol under sonication for 15 minutes (Sharma *et al.*, 2017). ZnO films deposited on the FTO substrate were then annealed at two different temperatures, first at 100°C for 30 minutes and then at 450° C for 2 hours.

These samples were characterized using XRD for structural analysis and Raman spectroscopy for optical stability. Bruker D2 Phaser diffractometer, operating at the voltage 30 kV and current 10 mA with X-ray wavelength of CuK_α (λ=1.54 Å) was employed for XRD analysis in the 2θ ranged from 0° to 80°. The band gap was calculated using the transmittance data captured by UV-visible spectrophotometer (Carry 60; Agilent Technologies). Ultimately, this paper reports the effect of KNO_3 salt in synthesis of ZnO NPs on DSSC performance by measuring the I-V characteristic curves using the Albet Solar Simulator under the illumination of the light of intensity 1000 Watt/m^2.

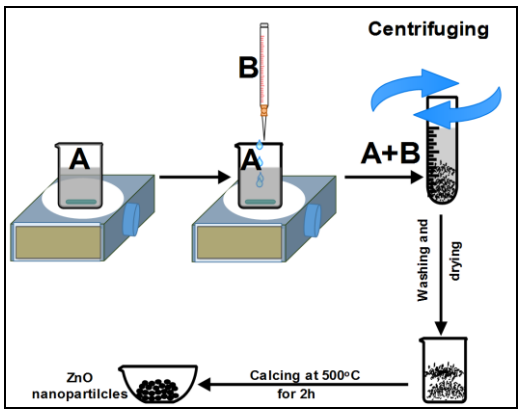

Fig. 1. A schematic diagram for preparation of ZnO nanoparticles

RESULTS AND DISCUSSION

XRD Analysis

The XRD patterns of ZnO NPs prepared with and without KNO_3 salt are shown in Figs 2(a) and 2(b), respectively. In both cases, the peaks of ZnO NPs were observed at 2θ = 31.84°, 34.44°, 36.24°, 47.55°, 56.76°, 62.97°, 66.47°, 68.01°, 69.18°, 72.68° and 76.98°. These peaks were indexed to (100), (002), (101), (102), (110), (103), (200), (112), (201), (004) and (202), respectively for ZnO in accordance with JCPDS cards 36-1451 and 89-1397. These observed multiple sharp diffraction peaks illustrate the good crystallinity of as-prepared ZnO NPs. No impurity phases have been observed. From this measurement, it was found that broad and relatively mild peaks were observed for ZnO prepared with KNO_3. In contrast, sharp and intense peaks were observed in ZnO NPs prepared without KNO_3. The apparent crystallite size (D) of ZnO was calculated by using Debye-Scherrer's equation (Cullity, 1977; Mulmi *et al.*, 2016).

$$D = \frac{K \times \lambda}{\beta \times \text{Cos}\theta} \quad (1)$$

Where, K is the shaping factor (the value 0.9 for ZnO), λ is the wavelength of X-ray used, β is full width at half maximum (FWHM) of the diffracted X-ray peak in radian, and θ is Bragg's angle (Dedova *et al.*, 2007).

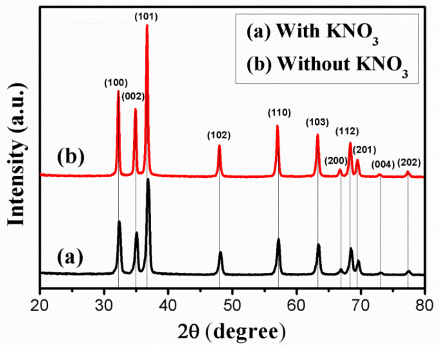

Fig. 2. XRD patterns of ZnO NPs synthesized with (a) and without (b) KNO_3 salt

Since the size and morphology of ZnO are important parameters in determining the physical and physicochemical properties of ZnO (Hu *et al.*, 2003), we have calculated the change in crystallite size of ZnO due to introduction of KNO_3 in the synthesis process. The calculated D corresponding to the most intense peak (101) of ZnO showed a decrease in size from 25 nm to 17 nm when potassium nitrate salt was added into the precursor solution, which was found to be consistent with results of Nejati *et al.* (2011). In the absence of KNO_3, adsorbed Zn^{2+} reacts with OH^- to form ZnO so that ZnO crystals show growth oriented along c-axis of hexagonal wurtzite structure. When KNO_3 is added into the precursor solution, the ZnO crystal undergoes structure evolution

due to competition of available K^+ ion with Zn^{2+} that inhibits the adsorption of Zn^{2+} on this plane, and forced more Zn^{2+} to be adsorbed onto the six side planes of wurtzite crystal structure of ZnO (Nejati *et al.*, 2011). The change in morphology was accompanied by change in size of ZnO NPs.

Raman spectroscopy of ZnO NPs

Further, to investigate the optical vibrational properties of the as-prepared ZnO NPs sample, Raman (EnSpectrRaPort Handheld Raman Analyzer-www.enspectr.com/products/raport-en) spectroscopic technique was applied. It utilizes a 30 µm entrance slit, 1800 g/mm holographic grating, cutting-edge low pass filter, as well as a 30 mW single-mode laser emitting at 532 nm to provide high accuracy Raman measurements in a broad spectral range from 90 to 4000 cm^{-1}. Fig. 3 shows the Raman spectrum of ZnO NPs prepared with KNO_3. The inset shows the clear presence of E_2 (high) at 437 cm^{-1} (Guo *et al.*, 2009; Fukushima *et al.*, 2017; Khan *et al.* 2015; Srivastava *et al.*, 2010). It has also been reported that the presence of dopants in the ZnO lattice can cause a significant shift in the Raman vibrational frequency of the E_2 (high) mode. According to the literature (Raymond *et al.*, 2017), the combination of acoustic phonons of the A_1+ E_2 is normally detected at about 1101 cm^{-1} in bulk ZnO samples. The Raman spectra of ZnO sample prepared by pneumatic spray pyrolysis technique showed a broad peak from 1017 cm^{-1} to 1207 cm^{-1} which was attributed to the multi-phonon modes (Raymond *et al.*, 2017).

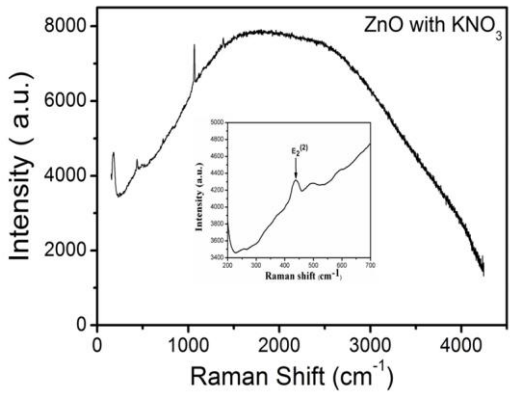

Fig. 3. Raman spectrum of ZnO NPs prepared with KNO_3 salt

Band gap of ZnO and absorbance of dye extract

The band gap of ZnO film was measured using the transmittance versus wavelength data captured by UV-visible spectrophotometer. In general, the absorption coefficient (α) is related to photon energy (hν) by the known equation as:

$$(\alpha h\nu)^{1/n} = \beta(h\nu - E_g) \quad (2)$$

Where, β is a constant called the band tailing parameter, E_g is the energy of the optical band gap, and n is the power factor of the transition mode, which is dependent upon the nature of the material. According to Tauc relation (Tauc & Menth, 1972), the plotting of $(\alpha h\nu)^2$ versus the photon energy (hν) gives a straight line in a particular region. The extrapolation of this straight line intercepts the (hν) axis to provide the value of the optical energy gap (Mulmi *et al.*, 2018). Fig. 4 depicts the Tauc plot of ZnO thin films. The calculated band gap energies of ZnO films prepared from ZnO NPs with and without KNO_3 were 3.16 eV and 3.26 eV, respectively, which lie in the range of reported value of ZnO (Al-Kahlout, 2015).

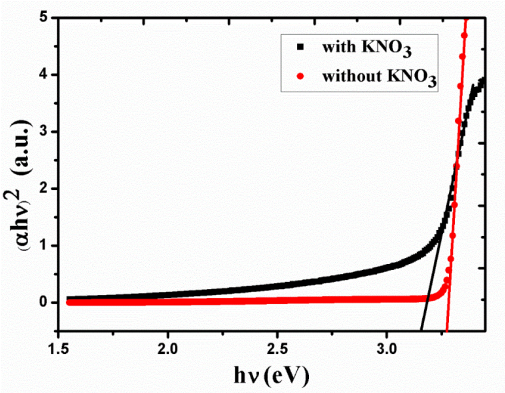

Fig. 4. Tauc plot to calculate the bandgap of ZnO film prepared from ZnO NPs with and without KNO_3

Fig. 5 shows the absorbance of *Artocarpus lakoocha* dye extract prepared in ethanol. It indicates wide absorbance in the visible range with three significant peaks at 280 nm, 465 nm and 656 nm. Hence this dye can absorb UV and visible light thereby increasing the efficiency of the DSSC.

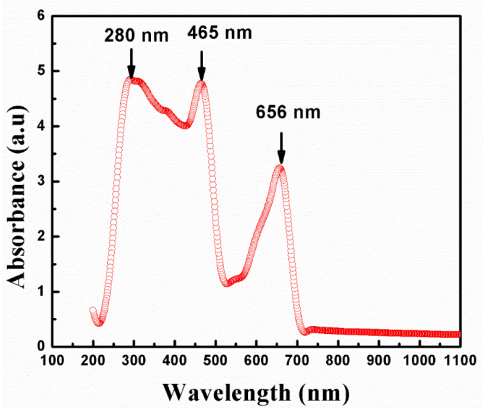

Fig. 5. The absorbance of dye extract of Artocarpus Lakoocha

DSSC performance

The performance of DSSC was tested by measuring I-V curves with Albet Solar Simulator (Bhandari *et al.*, 2017).

Fig. 6 shows the characteristic I-V curves of DSSCs prepared using ZnO films. The ZnO thin film was first sensitized by *Artocarpus lakoochadye* extract at 60° C for an hour and then I-V measurement was taken in the presence of intensity of light 1000 Watt/m^2. The red circle symbol represents the I-V plot of DSSC prepared from ZnO without additive, and black square symbol represents the I-V plot of DSSC from ZnO NPs prepared with additive KNO_3. The result showed higher values of short circuit current (I_{SC}) of 44 μA and open-circuit voltage (V_{OC}) of 326 mV. In conclusion, the presence of KNO_3 enhanced the surface area of ZnO film, which in turn helped in increasing the performance of DSSC.

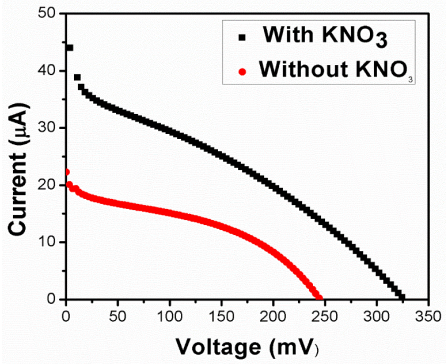

Fig. 6. I-V curves of DSSC fabricated from ZnO NPs with and without KNO_3

CONCLUSION

ZnO nanoparticle was successfully synthesized with and without KNO_3 from the precursor mixture of zinc acetate, and sodium hydroxide in ethanol solution by the precipitation method. All the XRD peaks were clear and sharp. This evidence proved that both ZnO NPs were well crystallized. Further, the XRD investigation of the effect of adding KNO_3 salt into the zinc acetate solution showed a decrease in crystallite size of ZnO NPs from 25 nm to 17 nm. The Raman analysis illustrated the presence of E_2 high peak at 437 cm^{-1} which confirmed the formation of stable wurtzite structured ZnO. From the optical absorption measurement, it was found that the band gap energy of ZnO NPs with and without KNO_3 were 3.16 eV and 3.26 eV, respectively. The current-voltage analysis of a dye-sensitized solar cell fabricated with photo-electrode prepared with small size ZnO NPs had shown enhancement in short circuit current and open-circuit voltage. The maximum observed I_{sc} and V_{oc} were of 44 μA and 326 mV, respectively, for ZnO prepared with KNO_3 salt.

ACKNOWLEDGEMENTS

The authors would like to thank Department of Physics, Amrit Campus and Tri-Chandra Campus of Tribhuvan University, Nepal Academy of Science and Technology (NAST), and Kathmandu University for providing research facilities to conduct this research work. One of the authors (DDM) is grateful to the TWAS research grant (RGA No.: 12-143 RG/PHYS_AS_I-UNESCO FR: 3240271367).

REFERENCES

Al-Kahlout, A. (2015). Thermal treatment optimization of ZnO nano-particles photo-electrodes for high photovoltaic performance of dye-sensitized solar cells. *Journal of the Association of Arab Universities for Basic and Applied Sciences*, *17*, 66-72.

Bhandari, S. C., Sharma, S., Shrestha, S. P., & Joshi, L. P. (2017). Preparation of ZnO thin films by hydrothermal method using Zn acetate with ethylene glycol precursor materials for dye-sensitized solar cell. *Imperial Journal of Interdisciplinary Research*, *3*(2), 920-924.

Chatterjee, A. P., Mitra, P., & Mukhopadhyay, A. K. (1999). Chemically deposited zinc oxide thin film gas sensor. *Journal of Materials Science*, *34*, 4225-4231.

Chen, Y. C., & Lo, S. L. (2011). Effects of operational conditions of microwave-assisted synthesis on morphology and photocatalytic capability of zinc oxide. *Chemical Engineering Journal*, *170*, 411-418.

Chu, J. B., Huang, S. M., Zhang, D. W., & Bian, Z. Q. (2009). Nano-structured ZnO thin films by chemical bath deposition in basic aqueous ammonia solutions for photovoltaic applications. *Applied Physics A, Materials Science & Processing*, *95*, 849-855.

Cullity, B. D. (1977). *Elements of X-ray diffraction* (2nd ed.). USA: Addison-Wesley Publ. Company, Inc., p. 101.

Dedova, T., Krunks, M., Grossberg, M., Volobujeva, O., & Acik, I. O. (2007). A novel deposition method to grow ZnO nano-rods: spray pyrolysis. *Superlattices and Microstructures*, *42*, 444-450.

EnSpectrRaPort Instrument manual, Enhanced Spectrometry, Inc. CA, USA. www.enspectr.com/products/raport-en

Fukushima, H., Uchida, H., Funakubo, H., Katoda, T., & Nishid, K. (2017). Evaluation of oxygen vacancies in ZnO single crystals and powders by micro-Raman spectroscopy. *Journal of Chemical Society of Japan*, *125*(6), 445-448.

Ghimire, R. R., Mondal, S., & Raychaudhuri, A. K. (2015). Synergistic ultraviolet photoresponse of a nanostructured ZnO film with gate bias and ultraviolet illumination. *Journal of Applied Physics*, *117*, 105705.

Ghorbani, H. R., Mehr, F. P., Pazoki, H., & Rahmani, B. M. (2015). Synthesis of ZnO nanoparticles by precipitation method. *Oriental Journal of Chemistry, 31*, 1219-1221.

Guo, S., Du, Z., & Dai, S. (2009). Analysis of Raman modes in Mn-doped ZnO nanocrystals, *Physica Status Solidi (b), 246*(10), 2329-2332.

Mulmi, D. D., Dahal, B., Kim, H.Y., Nakarmi, M. L., & Panthi, G. (2018). Optical and photo-catalytic properties of lysozyme mediated titanium dioxide nanoparticles. *Optik, 154*, 769-776.

Mulmi, D. D., Thapa, D., Dahal, B., Baral, D., & Solanki, P. (2016). Spectroscopic studies of boron doped titanium dioxide nanoparticles. *International Journal of Materials Science and Engineering, 4*(3), 172-178.

Nejati, K., Rezvani, Z., & Pakizevand, R. (2011). Synthesis of ZnO nanoparticles and investigation of the ionic template effect on their size and shape. *International Nano Letter, 1(2)*, 75-81.

Panthi, G., Ranjit, R., Kim, H. Y., & Mulmi, D. D. (2018). Size dependent optical and antibacterial properties of Ag_3PO_4 synthesized by facile precipitation and colloidal approach in aqueous solution. *Optik, 156*, 60-68.

Plank, S. O. V., Howard, I., Rao, A., Wilson, M. W. B., Ducati, C., Mane, R. S., Bendall, J. S., Louca, R. R. M., Greenham, N. C., Miura, H., Friend, R. H., Snaith, H. J., & Welland, M. E. (2009). Efficient ZnO nanowire solid-state dye-sensitized solar cells using organic dyes and core-shell nanostructures. *Journal of Physics Chemistry C, 113*, 18515-18522.

Ramimoghadam, D., Hussein, M. Z. B., & Taufiq-yap, Y. H. (2012). The effect of sodium dodecyl sulfate (SDS) and cetyl trimethyl ammonium bromide (CTAB) on the properties of ZnO synthesized by hydrothermal method. *International Journal of Molecular Science, 13*, 13275-13293.

Raymond, T., Luyolo, N., & Edson, M. (2017). Structural, morphological and Raman scattering studies of carbon doped ZnO nanoparticles fabricated by PSP technique. *Journal of Nanoscience and Nanotechnology Research, 1*, 1-8.

Sharma, S., Bhandari, S. C., Shrestha, S. P., & Joshi, L. P. (2017). Synthesis and study of ZnO nanoparticles for dye sensitized solar cell. *Research Journal of Physical Sciences, 5*(5), 6-10.

Srivastava, A. K., Praveen, Arora, M., Gupta, S. K., Chakraborty, B. R., Chandra, S., Toyoda, S., & Bahadur, H. (2010). Nanostructural features and optical performance of RF magnetron sputtered ZnO thin films. *Journal of Material Science Technology, 26*, 986-990.

Suh, D. -I, Lee, S. -Y., Kim, T. -H, Chun, J. -M., Suh, E. -K., Yang, O. -B., & Lee, S. -K. (2007). The fabrication and characterization of dye-sensitized solar cells with a branched structure of ZnO nanowires. *Chemical Physics Letters, 442*, 348-353.

Tauc, J. & Menth, A., (1972). States in the gap. *Journal of Non-Crystalline Solids, 8-10*, 569-585.

Wang, Z., Zhang, H. Zhang, L., Yuan, J., Yan, S., & Wang, C. (2003). Low-temperature synthesis of ZnO nanoparticles by solid-state pyrolytic reaction. *Nanotechnology, 14*, 11-15.

Yadav, R. S., Mishra, P., & Pandey, A. C. (2008). Growth mechanism and optical property of ZnO nanoparticles synthesized by sonochemical method. *Ultrasonics Sonochemistry, 15*, 863-868.